Thesis for the degree
Master of Science

Submitted to the Scientific Council of the
Weizmann Institute of Science
Rehovot, Israel

עבודת גמר (תזה) לתואר
מוסמך למדעים

מוגשת למועצה המדעית של
מכון ויצמן למדע
רחובות, ישראל

By
Dana Raiter

מאת
דנה רייטר

אנליזה משולבת של שיטה אוילרית ולגראנג׳ית של הסירקולציה האטמוספרית בטרופים וההשלכות על שינויי אקלים

A coupled Eulerian-Lagrangian analysis of the large-scale tropical atmospheric circulation and its implication for climate change

Advisor:
Prof. Yohai Kaspi

מנחה:
פרופ׳ יוחאי כספי

December 2020

כסלו ה׳תשפ״א

Abstract

The Hadley circulation is a key element of the climate system. It is traditionally defined as the zonally averaged meridional circulation in the tropics, therefore treated as a zonally symmetric phenomenon. However, differences in temperature between land and sea cause zonal asymmetries on Earth, dramatically affecting the circulation. This longitudinal dependence of the meridional circulation evokes questions about where and when the actual large scale tropical circulation occurs. Here, we look into the connection between the longitudinally dependent meridional circulation, and the actual large scale transport of air in the tropics using a coupled Eulerian and Lagrangian approach. Decomposing the velocity field into rotational and divergent components, we identify how each component affects the actual circulation. We propose an alternative definition for the circulation, that describes the actual path of air parcels in the tropics, as a tropical atmospheric conveyor belt. We further investigate this definition, analyzing the circulation under climate change and its effect on precipitation changes. We show that in order to predict future climate, the regionality and three-dimensionality of the large-scale tropical circulation must be taken into account. We find that the changes in the circulation vary significantly over longitude, and are overlooked when analyzing the zonally averaged meridional circulation. The circulation is strengthening and expanding in the center of the Pacific, a region where the circulation barely existed in past. On the other hand, the circulation is weakening in the Indo-Pacific region, where it was the most significant in the past. These differences appear as a shift in the region of ascent of the conveyor belt, that is revealed when analyzing the decomposed vertical wind. The pattern of weakening of the ascent in the Indo-Pacific and strengthening in the center of the Pacific explains the projected changes in precipitation. The Indo-Pacific region is drying, while the precipitation in the center of the Pacific is intensifying.

Acknowledgements

I would like to express my gratitude to Professor Yohai Kaspi who guided me throughout my studies. His enthusiasm and devotion to his students inspired and encouraged me to pursue a career in science. I would like to thank Dr. Eli Galanti, who advised me throughout my studies and introduced me to my undergraduate research project that led to my thesis and became my primary research interest. I would like to express my appreciation for their time, dedication, and mentorship in my research and studies as well as assisting me with my PhD application. I would like to thank Rei Chemke for his help and suggestions for analyzing the climate change simulations and for answering all my questions. I would also like to thank my group members: Keren Duer, Nimrod Gavriel, Maria Smirnova, Or Hadas, Ilai Guendelman, and Orli Lachmy for their support, advice, and making my workdays at the office enjoyable. I would like to thank the administrative staff at the department of Earth and Planetary Sciences, for their help with anything I needed during my studies in the department. Finally, I would like to thank my family and my partner, Assaf, for their endless support and encouragement.

Table of Contents

List of Figures

Chapter 1

Introduction

The Hadley circulation (HC) is responsible for the majority of the heat transport in the tropics, and is strongly tied to many phenomena including the trade winds, the subtropical deserts, and the subtropical jet-streams (Hartmann, 2016). The importance of the HC stimulated countless studies on the mechanisms controlling the circulation and its temporal variability (e.g., Held and Hou, 1980; Lindzen and Hou, 1988; Dima and Wallace, 2002). The HC is traditionally defined as the zonally averaged meridional circulation (Vallis, 2006), overlooking the zonal asymmetry on Earth and therefore creating a two dimensional perception of the circulation. The traditional definition has proven very useful for understanding the phenomenon and its variability. Many studies have been conducted about the variability of the zonally averaged meridional circulation in past and present times, as well as for the future, under climate change (e.g., Diaz and Bradley, 2004; Chemke and Polvani, 2019a). Others used the traditional definition for theoretical understanding of the HC. For example, Held and Hou (1980) introduced a theory that explains the width of the HC making several assumptions, including zonal symmetry. However, differences in temperature between land and sea cause variability in observations at different longitudes, leading to a more complex structure of the HC in reality. This led to a more local analysis of regional and seasonal aspects of the HC, by analyzing, for example, the vertical and meridional velocities as function of latitude and longitude, and trajectories of the climatological flow emphasizing the regional aspects of the HC (Karnauskas and Ummenhofer, 2014).

A different approach is to decompose the velocity field into rotational and divergent components (Helmholtz decomposition), and then by using only the divergent component of the flow, the localized meridional circulation can be calculated (Keyser et al., 1989). Schwendike et al. (2014) used this decomposition method to calculate the relative contributions of the vertical mass fluxes in the middle-troposphere to the Hadley and Walker circulations. The same method was also used to study specific regions of interest, such as the Atlantic sector of the HC during the Boreal summer and its connection to the Atlantic tropical cyclone activity (Zhang and Wang, 2013), and the variability of the HC in the Southern Hemisphere in different sectors of the world (Nguyen et al., 2018). The same methodology was used to study the inter-decadal trend of both the Hadley and Walker circulations, where it was shown that in order to under-

stand the effect of climate variability on the tropical circulation patterns, the analysis should be regional (Schwendike et al., 2015).

The decomposition into the divergent and rotational components is very useful for understanding the longitudinal variations of the meridional circulation, helping to locate where the circulation occurs. However, analyzing one component of the circulation gives an incomplete picture that does not represent the actual flow. The velocity field is constructed from all components, and therefore it is necessary to understand the effect of each component on the flow. Moreover, even when analyzing all components, it is impossible to obtain the actual movement of the air in the atmosphere using this Eulerian approach, since the combined effect of all components is not apparent when observing each component separately. Therefore, an analysis of the actual movement of air is required, one that captures and visualizes the contribution of all the components together.

This analysis is critical when examining the tropical circulation under climate change. Numerous studies address the past changes in the HC since 1979, concluding that the HC has been expanding at a rate of $\sim 0.2^{\circ}$ per decade (e.g., Davis and Rosenlof, 2012; Seidel and Randel, 2007; Hu and Fu, 2007; Grise et al., 2019; Staten et al., 2018; Chemke and Polvani, 2019b). This expansion is expected to continue throughout the twenty-first century due to the increase of greenhouse-gas emissions (e.g., Lu et al., 2007; Nguyen et al., 2015; Waugh et al., 2018; Staten et al., 2012).

Previous studies on the HC expansion used various methods and took into consideration multiple factors which might affect the rate of expansion. For example, analyzing different metrics for the definition of the HC edge (Waugh et al., 2018), or studying the effect of multiple forcing mechanisms on simulated expansion of the HC (Staten et al., 2012), and examining uncertainties in future trends of the HC width due to internal variability (Kang et al., 2013). Other studies examined the mechanisms that explain this expansion (e.g., Chemke and Polvani, 2019a). What most of these studies have in common is that they use the traditional definition of the HC, the zonally averaged meridional circulation. However, the expansion of the HC varies significantly over longitude (Staten et al., 2019; Lucas, 2015).

The Helmholtz decomposition allows to analyze the changes in the HC at all longitudes. Staten et al. (2019) applied the decomposition method on reanalyses data, as well as forced and unforced model simulations and showed that while the weakening of the HC with increase of greenhouse-gases is robust, the widening of the circulation occurs in specific regions, where it is less significant. Furthermore, when investigating the time-of-emergence (ToE) of the expansion of the northern hemisphere HC, only in the Middle East/Mediterranean region is the ToE found to occur before the end of the 21^{st} century (D'Agostino et al., 2020), again underlining the regionality of the circulation.

These results emphasize the importance of considering the longitudinal variability of the HC to accurately predict the changes. Yet, analyzing only one component of the velocity field yields a two-dimensional perspective of the circulation, overlooking the fact that the actual flow in the atmosphere is three-dimensional and affected by all components of the velocity field

(Raiter et al., 2020). Moreover, different phenomena that emerge in different dimensions such as the subtropical jet stream and the HC are known to be physically connected (Held and Hou, 1980), however, recent studies found poor correlation between variations in the location of the edge of the HC and the location of the subtropical jet-stream (Waugh et al., 2018; Davis and Birner, 2017; Menzel et al., 2019).

Lastly, another manifestation of the regionality of the circulation is observed in the precipitation change under global warming. The connection between the Hadley circulation and precipitation is well established and past studies even used the precipitation change as indication of Hadley cell expansion (Lu et al., 2007). Previous studies have suggested a few mechanisms for the response of the tropical atmospheric circulation to climate change and its affect on the hydrological cycle. In a review paper Ma et al. (2018) described these mechanisms among them the wet-get-wetter concept, which explains the large-scale changes in precipitation. This concept includes two hypothesis, the first by Held and Soden (2006), which assumes an insignificant change in the circulation, implying that the increased transport of moisture from dry regions to wet regions is due to increase in atmospheric water vapor, caused by warming. The increased transport of moisture leads to larger gradient of P-E (evaporation minus precipitation) between wet regions and dry regions. The second hypothesis is a dynamical feedback related to the gross moist stability. The gross moist stability is the export of moist static energy (MSE) from a tropospheric column by the mean circulation per unit of mean upward mass flux (Neelin and Held, 1987; Back and Bretherton, 2006). MSE is the combination of the internal energy, energy for expansion, potential energy and the latent heat of an air parcel. In other words, gross moist stability is a measure of the efficiency of the export of MSE by the large-scale circulation associated with moist convection. Low gross moist stability indicates a region of less stability, where stronger vertical velocities are required to export the MSE. In global warming simulations the gross moist stability is increasing in the tropics, meaning the atmosphere is more stable. This coincides with the weakening of the circulation under climate change (Chou et al., 2013).

The wet-get-wetter hypotheses assume a spatially uniform sea surface temperature (SST), however, the changes in SST have significant spatial variations (Xie et al., 2010), and therefore a regional analysis is of extreme importance. The regional response of the hydrological cycle was separated in previous studies to thermodynamical and dynamical mechanisms (e.g., Seager et al., 2010; Chadwick et al., 2013). This decomposition highlights the significant contribution of the dynamical component to the change in precipitation, in particular, the weakening of the circulation that opposes the thermodynamical mechanisms in some regions. These studies used the traditional definition of the zonal mean meridional circulation, and referred to any zonal asymmetry as part of the Walker circulation (Seager et al., 2010; Vecchi and Soden, 2007). Therefore, when discussing the contribution of the dynamical component to the changes in precipitation, zonally asymmetric dynamical changes were attributed to the weakening of the Walker circulation alone. The variations in the circulation were connected to regional SST patterns (Ma and Xie, 2013).

These results emphasize the need for a regional and three-dimensional analysis of the changes in the tropical large-scale circulation and their impact on the precipitation change under global warming.

Chapter 2

Goals

In this thesis, we investigate the longitudinally dependent large-scale tropical circulation using a coupled Eulerian and Lagrangian approach. Taking the Eulerian approach of using the Helmholtz decomposition method, and calculating the climatological meridional circulation at each longitude, combined with the Lagrangian approach of tracking air parcels in the atmosphere, allows to understand the actual movement of air associated with the large-scale tropical circulation. Our goal, using this combined approach is to develop a complete and global picture of the large-scale tropical three-dimensional circulation.

In addition, we investigate the response of the three-dimensional large-scale atmospheric circulation to anthropogenic warming by analyzing projected changes in the decomposed circulation under climate change. Similar to the analysis of observational data, we analyze trajectories of air parcels using forced and unforced simulations in order to obtain a full picture of the expected changes in the actual movement of air. We show examples for trajectories initially located in different regions, showing the localized variations of the circulation, resulting in very different responses of the air flow.

Finally, we use the decomposition of the vertical velocity associated with the meridional and zonal circulation to highlight specific regions where the circulation seems to be a significant contributor to the precipitation changes during climate change, further emphasizing the regionality of the circulation and its response to climate change.

Chapter 3

Methods

In this study we use a combination of Eulerian and Lagrangian approaches. Using the Eulerian approach, we decompose the velocity field and examine the different components of the circulation. Using the Lagrangian approach, we track air parcels in the atmosphere and examine the actual 3D motion of air parcels in the tropics. Combining the two analyses we create an understanding of the spatial variations of the components of the circulation and their contribution to the actual movement of air parcels in the atmosphere.
We start with analyzing the present large-scale circulation. To do so, we use the European Center for Medium Range Weather Forecasts ERA-Interim reanalysis data covering the years 1979-2018 (Dee et al., 2013).

3.1 Decomposition of the velocity field: Eulerian approach

Using the Helmholtz decomposition (e.g., Keyser et al., 1989; Schwendike et al., 2014; Hu et al., 2017) the observed velocity field can be decomposed into rotational and divergent components. Following the notation of Hu et al. (2017), the horizontal divergence of the wind is

$$D = \nabla \cdot \mathbf{v}, \tag{3.1}$$

where $\mathbf{v} = (u, v)$ is the horizontal wind vector, and the divergence is taken on constant pressure surfaces. Then, a potential function χ is calculated via

$$\nabla^2 \chi = D. \tag{3.2}$$

This potential represents only the divergent part of the horizontal flow, and therefore it can be used to calculate the divergent wind

$$\nabla \chi = \mathbf{v}_{\text{div}}, \tag{3.3}$$

where $\mathbf{v}_{\text{div}} = (u_{\text{div}}, v_{\text{div}})$. This velocity field satisfies the continuity equation: $\nabla \cdot \mathbf{v}_{\text{div}} + \frac{\partial \omega}{\partial p} = 0$. Finally, the divergent wind can be used to calculate the longitudinally dependent meridional

circulation

$$\psi(\phi,\theta,p,t) = \frac{1}{g}\int_0^p v_{\mathrm{div}}(\phi,\theta,p',t)dp', \tag{3.4}$$

where ϕ, θ, p and t are the longitude, latitude, pressure, and time, respectively, and g is the gravitational acceleration. Similarly, using u_{div} (u_{rot}) the zonal (rotational) circulation can be calculated. The zonal circulation is calculated via

$$\psi_{\mathrm{W}}(\phi,\theta,p,t) = \frac{1}{g}\int_0^p u_{\mathrm{div}}(\phi,\theta,p',t)dp'. \tag{3.5}$$

The horizontal circulation is calculated via

$$\psi_{\mathrm{R}}(\phi,\theta,p,t) = -a\int_0^p u_{\mathrm{rot}}(\phi,\theta',p,t)d\theta', \tag{3.6}$$

where a is the radius of the Earth.

For decomposing the vertical velocity into a meridional (ω_θ) and zonal (ω_ϕ) component, we follow the notation in Schwendike et al. (2014). Starting with calculating a potential function μ via

$$\nabla^2\mu = -\omega. \tag{3.7}$$

Then using the potential function we calculate ω_θ and ω_ϕ

$$\omega_\theta \sin\theta = \frac{1}{a^2}\frac{\partial}{\partial\theta}\left(\sin\theta\frac{\partial\mu}{\partial\theta}\right),\ \omega_\phi \sin\theta = \frac{1}{a^2\sin\theta}\frac{\partial^2\mu}{\partial\phi^2}. \tag{3.8}$$

The meridional component (ω_θ) participates in the meridional circulation, therefore is coupled with the divergent component of the meridional wind (v_{div}), while the zonal component (ω_ϕ) participates in the zonal circulation and is coupled with the divergent component of the zonal wind (u_{div}).

3.2 Calculating trajectories of air parcels: Lagrangian approach

For the Lagrangian analysis we use LAGRANTO (Sprenger and Wernli, 2015), a Lagrangian analysis tool which calculates trajectories of air parcels. The Lagranto calculations are based on netCDF files containing 3-D wind fields. The tool numerically solves the trajectory equation: $\frac{D\boldsymbol{x}}{Dt} = \boldsymbol{u}(\boldsymbol{x})$ with a number of iterative steps. The code receives as input the starting time t and starting position $\boldsymbol{x}$. For the first step it calculates a new position $\boldsymbol{x}^*$ at time $t + \Delta t$, in our case Δt equals 6 hours:

$$\boldsymbol{x}^* = \boldsymbol{x} + \boldsymbol{u}(\boldsymbol{x},t)\Delta t. \tag{3.9}$$

Before the second iteration, the wind vector is averaged between the wind values at the starting position and the wind values at the estimated new position:

$$\boldsymbol{u}^* = \frac{1}{2}\left[\boldsymbol{u}(\boldsymbol{x}, t) + \boldsymbol{u}(\boldsymbol{x}^*, t + \Delta t)\right]. \tag{3.10}$$

Therefore, in the second iteration the new position is obtained by:

$$\boldsymbol{x}^{**} = \boldsymbol{x} + \boldsymbol{u}^*(\boldsymbol{x}, t)\Delta t. \tag{3.11}$$

Further details can be found in Sprenger and Wernli (2015).

3.3 Analyzing climate change model simulations

For analyzing variations of the circulation under climate change we use a multi-model mean of the Coupled Model Intercomparison Project phase 5 (CMIP5, Taylor et al., 2012). We present analysis of the historical data for the years 1960-1999 and forced by the Representative Concentration Pathway 8.5 (RCP 8.5) emissions scenario for the years 2060-2099.

For the Eulerian analysis we average the velocity field of 17 CMIP5 models (listed in Table. 3.1) for historical and RCP 8.5 simulations. The edge of the zonally averaged HC is represented by the latitude of the zero crossing of the mean meridional circulation at 500 hPa. In order to avoid biases caused by ill-defined velocity fields, we place a NaN everywhere in the data where wind cannot exist (i.e., underground). Where the decomposed circulation is presented (Fig. 5.3) the edge of the meridional and zonal circulation is defined as the contour of the 20% of the maximum or minimum value of each field at 500 hPa. Statistical significance is calculated using the Student's t test, at a confidence level of 95%.

Applying the Lagrangian approach, we track air parcels using an average of a subset of 8 CMIP5 models from the 17 we used for the Eulerian analysis (Table 3.1, marked with asterisk), for the historical and RCP 8.5 simulations. We only use models that are originally fully defined in the vertical direction in order to maintain continuity of the trajectories. The Lagranto tool is not designed to work on CMIP5 data, therefore, we calculated the trajectories using Eq. 3.9, which gives very similar results to the Lagranto calculation. Note that the mean meridional circulation presented in Fig. 5.2 is calculated with the same 8 models used for the Lagrangian analysis, for presenting the well-known picture of the HC in all the pressure levels).

Model	**Modeling Center**	**Atmospheric Resolution (lon x lat)**
ACCESS1.3	Commonwealth Scientific and Industrial Research Organization (CSIRO) and Bureau of Meteorology (BOM), Australia	$1.875° \times 1.25°$
BCC-CSM1.1*	Beijing Climate Center, China Meteorological Administration	$2.8125° \times 2.7906°$
BNU-ESM*	Beijing Normal University, China	$2.8125° \times 2.7906°$
CCSM4	National Center for Atmospheric Research	$1.25° \times 0.9424°$
CMCC-CM*	Euro-Mediterranean Centre on Climate Change, Italy	$0.75° \times 0.7484°$
CMCC-CMS*	Euro-Mediterranean Centre on Climate Change, Italy	$3.711° \times 3.75°$
CNRM-CM5	Centre National de Recheches Meteorologiques	$1.40624° \times 1.4008°$
CanESM2*	Canadian Centre for Climate Modelling and Analysis	$2.8125° \times 2.7906°$
FGOALS-g2	LASG, Institute of Atmospheric Physics, Chinese Academy of Sciences and CESS, Tsinghua University	$2.8125° \times 2.7906°$
FIO-ESM*	The First Institute of Oceanography (FIO), SOA, China	$2.8° \times 2.8°$
GFDL-CM3	NOAA GeophysicalFluid Dynamics Laboratory	$2.5° \times 2°$
GISS-E2-R	NASA Goddard Institute for Space Studies	$2.5° \times 2°$
MIROC-ESM-CHEM	Atmosphere and Ocean Research Institute (The University of Tokyo), National Institute for Environmental Studies, and Japan Agaency for Marine-Earth Science and Technology	$2.8125° \times 2.7906°$
MIROC5	Atmosphere and Ocean Research Institute (The University of Tokyo), National Institute for Environmental Studies, and Japan Agaency for Marine-Earth Science and Technology	$1.40625° \times 1.4008°$
MPI-ESM-LR*	Max Planck Institute for Metorology	$1.875° \times 1.8653°$
MPI-ESM-MR*	Max Planck Institute for Metorology	$1.875° \times 1.8653°$
MRI-CGCM3	Meteorological Research Institute	$1.125° \times 1.12148°$

Table 3.1: List of the 17 CMIP5 models analyzed in this study, and their atmospheric resolutions. Asterisks mark the subset of 8 models used for the Lagrangian analysis.

Chapter 4

Results- reanalysis data

4.1 Eulerian analysis

From the latitudinally dependent meridional circulation, ψ (Eq. 3.4), we reproduce the classic double HC by calculating its zonal and time average over all years (Fig. 4.1a). The circulation is found to be most intense between 400 and 600 hPa. Averaging ψ between 400 and 600 hPa, and presenting the circulation as function of latitude and month of the year (Fig. 4.1b), the well known seasonal cycle emerges, reaching maximum values in January (Northern Hemisphere (NH) winter) and July (Southern Hemisphere (SH) winter). The climatology of the longitudinally dependent circulation in July is obtained by averaging ψ between 400 and 600 hPa as well as time averaging over all the July months between 1979-2018 (Fig. 4.1c). In this description air is rising and descending in the white areas. The ascending (descending) branch goes north (south) for orange (blue) contours and south (north) for blue (orange) contours. The variability in longitude is very prominent (Fig. 4.1c) with a strong cell between 50°E and 150°W. Between 160°W and 60°W there is a much smaller and far weaker cell. In other words, the circulation in the tropics is, in fact, not zonally symmetric prompting the need to take into account its longitudinal dependence.

Following the same steps, we calculate, using u_{div}, the latitudinally dependent zonal (Walker) circulation (Fig. 4.1d), and the rotational circulation using u_{rot} at 200 hPa and 850 hPa (Fig. 4.1e-f). It is apparent that all circulations have strong spatial variations, and each component affects the actual motion of air in the atmosphere. For example, the strong ascent in the West Pacific participates in both the meridional and zonal circulations there. The rotational components contribute to the movement only in the horizontal direction, which will not be captured when examining only the meridional circulation. Thus, in order to understand what dominates the movement of air in the tropical atmosphere, we need to analyze the magnitude and direction of each component and its contribution to the overall circulation.

In the meridional circulation in January, similarly to July, we see strong longitudinal variations (Fig. 4.2c) with one significant cell between 50°E and 150°W and a smaller cell between 70°W and 50°W. In January, the zonal circulation in the Pacific Ocean (Fig. 4.2d), which its ascending branch goes east, is more intense than the zonal circulation found in the Indian

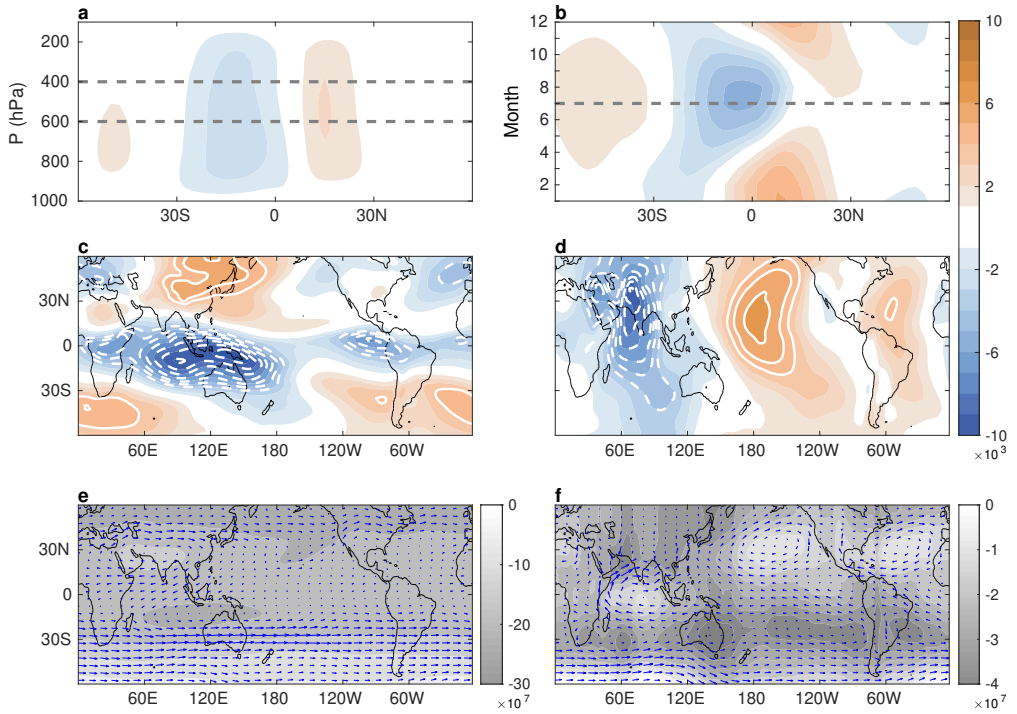

Figure 4.1: (a) The annually and zonally averaged meridional circulation as function of latitude and pressure, with the dashed lines denoting the 400 and 600 hPa levels. (b) The zonal mean meridional circulation, averaged between 400-600 hPa, as function of latitude and month of the year, with the dashed line denoting July. (c-f) The time average of the different components of the circulation in July as function of Longitude and Latitude. (c) The meridional circulation and (d) the zonal circulation, both averaged between 400 and 600 hPa. (e) The rotational circulation at 200 hPa and (f) the rotational circulation at 850 hPa. Arrows indicate the rotational component of the horizontal velocity. For (a-d): contour interval is $1 \times 10^3\,\mathrm{kg\,s^{-1}m^{-1}}$, and white solid and dashed lines indicate absolute values larger than $4 \times 10^3\,\mathrm{kg\,s^{-1}m^{-1}}$. For (e-f): colored contours are in units of $\mathrm{m^2 s^{-1}}$. Note that the traditional mass streamfunction, given in $\mathrm{kg\,s^{-1}}$ can be obtained by multiplying (a-c) by a factor of $2\pi a \cos\theta$.

Ocean, which its ascending branch goes west. On the other hand, in July, the pattern is exactly the opposite, with strong circulation in the Indian Ocean, and a weaker one in the Pacific (Fig. 4.1d). The rotational circulation at 200 hPa (Fig. 4.1e, 4.2e) and the horizontal velocity show the jet stream in both seasons in the winter hemisphere.

4.2 Lagrangian analysis

4.2.1 Mean flow trajectories

The Eulerian analysis, exposing the distinct spatial patterns of the circulation, prompts several questions: what does the real movement of air in the tropics look like, and how is it connected to the patterns? What is the typical time scale of this motion, and is the air involved in the circulation confined to the tropics? To answer these questions, we use Lagranto (Sprenger and Wernli, 2015). Using the climatological flow for July and January we calculate representative trajectories for each month (Fig. 4.3). In each of them, we follow a total of 52 trajectories for

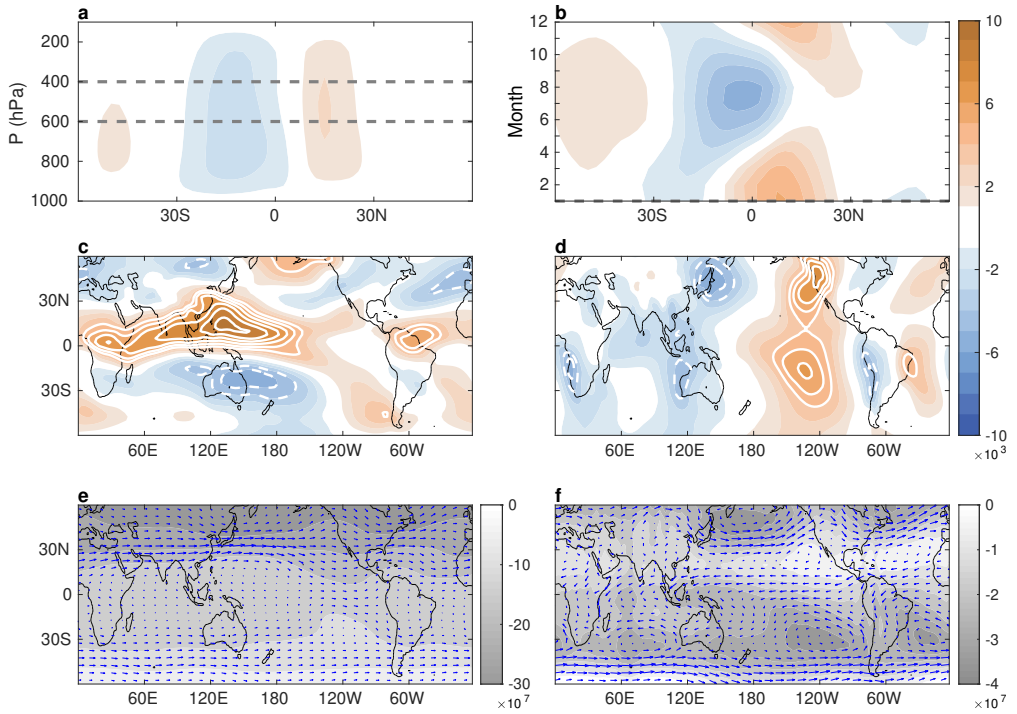

Figure 4.2: Same as Fig. 4.1, for January.

20 days. The initial locations of air parcels are selected where there is a strong ascent near the equator at a height of 500 hPa (black dots), corresponding to the strongest north-south shear in the dominant meridional overturning circulation. This ascent is also evident in the vertical velocity (Fig. 4.4). In the next analysis we discuss trajectories of air parcels with different initial positions, and further demonstrate why the Indo-Pacific is the main area of interest (Fig. 4.5).

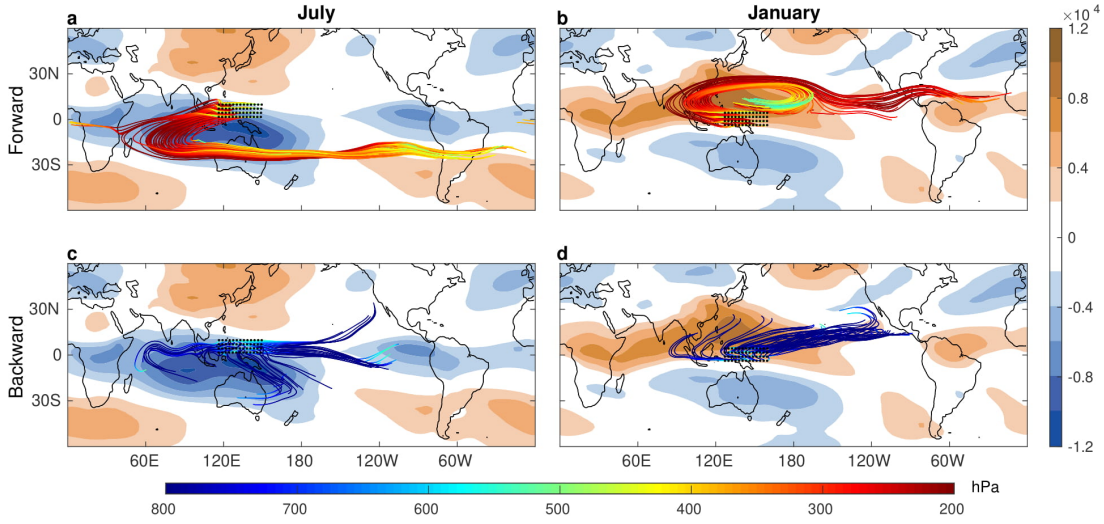

Figure 4.3: Mean flow trajectories and meridional circulation for July (left) and January (right). Shown is the meridional circulation at 500 hPa (contours), with contour interval of $2 \times 10^3\,\mathrm{kg\,s^{-1}m^{-1}}$. The lines show the air parcels trajectories going 20 days forward (a,b) and 20 days backward (c,d) in time. The initial locations are marked with black dots. The color of the lines indicates the pressure level in hPa (bottom colorbar).

The meridional circulation is easily identified in both months (Fig. 4.3), with the air rising locally near the equator, moving south in July and north in January and then descending.

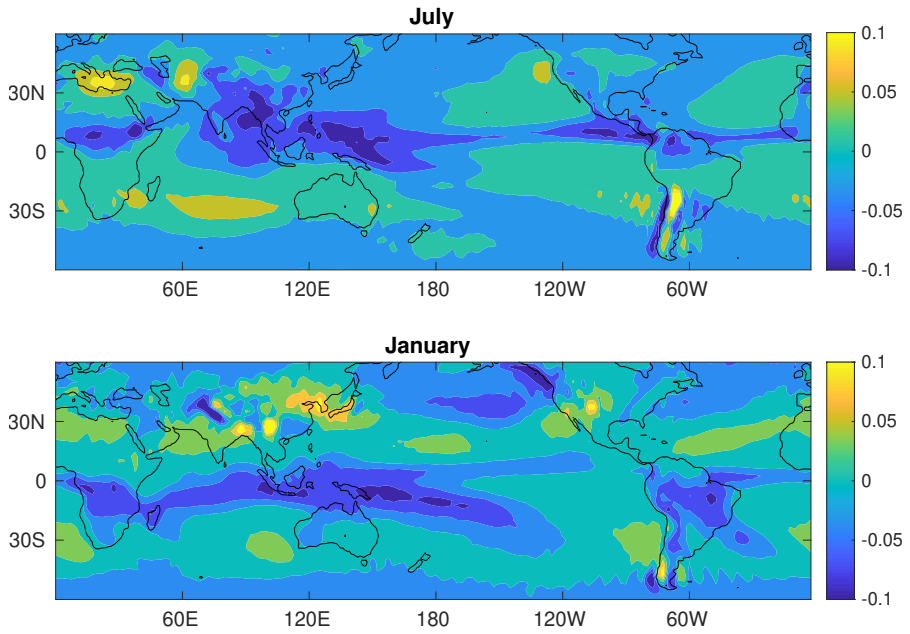

Figure 4.4: The climatological vertical wind at 500 hPa for July and January in $\mathrm{Pa\,s^{-1}}$.

However, in addition to this movement there is a strong movement in the east-west direction. Hence, the 3D movement of the air parcels needs to be described taking into account all the different components of the velocity field (Fig. 4.1c-f), in addition to the longitudinally dependent meridional circulation. It appears that in July, air parcels ascend mostly locally, move west due to the rotational component of the horizontal velocity, and then move south due to the meridional circulation (Fig. 4.3a). When the air parcels reach approximately 25°S they merge into the jet-stream (at its equatorial side) and move eastward rapidly, eventually descending near the Americas. In January, the picture is somewhat more elaborate because of the more complex continental configuration in the NH (Fig. 4.3b). However, the main path is still visible, with air rising locally and moving slightly west and then to the north. When the air parcels reach the jet-stream, approximately half of them move eastward with the jet and stay at high altitudes even after 20 days. The other half of the air parcels, which reach the southern boundary of the jet-stream, start to descend and veer west with the trade winds. In order to complete the analysis of the circulation, we calculate also the back trajectories for January and July, starting from the same initial positions (Fig. 4.3c,d). The movement of air parcels takes place mostly at lower altitudes, therefore the movement is slower. In both July and January, easterlies generate convergence of air parcels from the East Pacific to the starting positions. In July the air parcels appear to converge from the West Pacific as well, moving with the Walker circulation and with the rotational component of the horizontal wind at low altitudes.

4.2.2 Density of trajectories

The trajectories of the climatological flow, while useful for understanding the dominating path of air parcels, do not accurately represent the movement of air in reality, because the flow field is averaged in time, and variability and localized movement is lost. To address this

issue, we calculate the trajectories of air parcels without averaging over time, maintaining the variability. In order to visualize these trajectories, we calculate their spatial density. First, we define the region of initial positions of air parcels, by selecting a region of high rainfall, with more than 6 mm/day in the climatological convective precipitation (Fig. 4.5, black contour in upper panels). This region exhibits strong convection, associated with the ascending branch of the meridional circulation (ITCZ). We then calculate the trajectories of air parcels initially positioned in this region, using the 6-hourly data from Era-Interim for every July from 1979 to 2018. In total, we follow over 2000 starting positions and 4800 starting times, resulting in millions of air parcels. Next, we mark each air parcel's position every 6 hours, creating a distribution plot of all parcels without averaging over time.

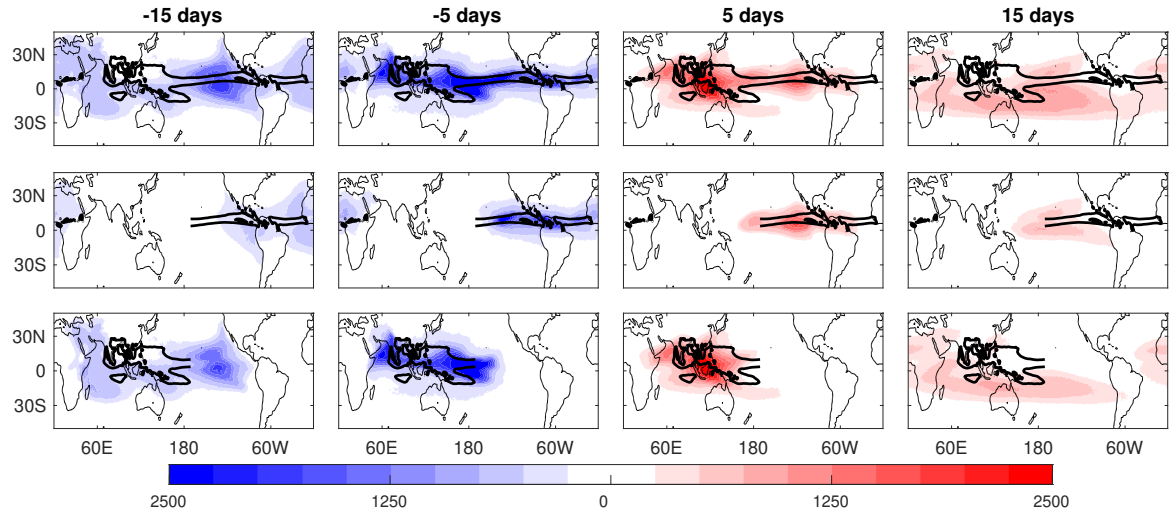

Figure 4.5: Distribution of air parcels in different sectors for all July months during 1979-2018. The black contour marks air parcels' initial position at 500 hPa, and the density of air parcels (number of parcels per a $1° \times 1°$ grid box) is marked in red for forward trajectories and blue for backward trajectories. The top row shows the density of all tracked air parcels, the middle row shows parcels initially located in the East Pacific and Atlantic Oceans and the bottom row shows parcels initially located in the Indo-Pacific. Shading indicates the relative number of air parcels at the specific location and time.

Fig. 4.5 shows the distribution of air parcels at -15, -5, 5 and 15 days relative to the time of initiation of the parcels in July. The top panels show all air parcels initially positioned at the high convection zone. The main path of air parcels visualized above (Fig. 4.3a,b) is clearly visible here. Air parcels move westward after 5 days, and after 15 days the movement south and eastward becomes prominent. In order to further clarify the movement of the air parcels, we separate the starting locations into two regions. The middle and bottom panels of Fig. 4.5 show air parcels initially positioned in the East Pacific and Atlantic Ocean, and in the Indo-Pacific region, respectively. The East Pacific and Atlantic air parcels show a rather confined movement, corresponding to the smaller and weaker overturning cell exhibited in the longitudinally dependent meridional circulation at the same location (Fig. 4.1c). The Indo-Pacific air parcels (bottom panels), on the other hand, participate in the circulation as it is defined with strong movement to the west, and later to the south and to the east. Hence, the Indo-Pacific region acts as the engine of the large-scale tropical circulation.

Distribution of back trajectories (Fig. 4.5, left panels) explains where the air parcels that participate in the circulation come from. In the East Pacific and Atlantic region (middle row) we see localized movement yet again, since these air parcels do not participate in the circulation. The air parcels converging into the Indo-Pacific region (bottom), however, reveal a few interesting features. First, as expected, air parcels converge into the Indo-Pacific from the East Pacific with the trade winds. Second, air parcels come also from the Indian Ocean, moving east. Third, while it would be expected that air parcels return mostly from the south, where they reach after 15 days, there is a symmetry between the NH and the SH, i.e., air parcels from both hemispheres converge into the Indo-Pacific. Although a closure of the circulation is not entirely apparent, it seems that 30 days is approximately the typical time scale of the circulation, since during this span, air parcels converge and diverge. Lastly, the air parcels are confined between approximately 30°S and 30°N, the limits of the traditionally defined HC. Although it is less recognizable than in July, the main path of the air parcels is identified in

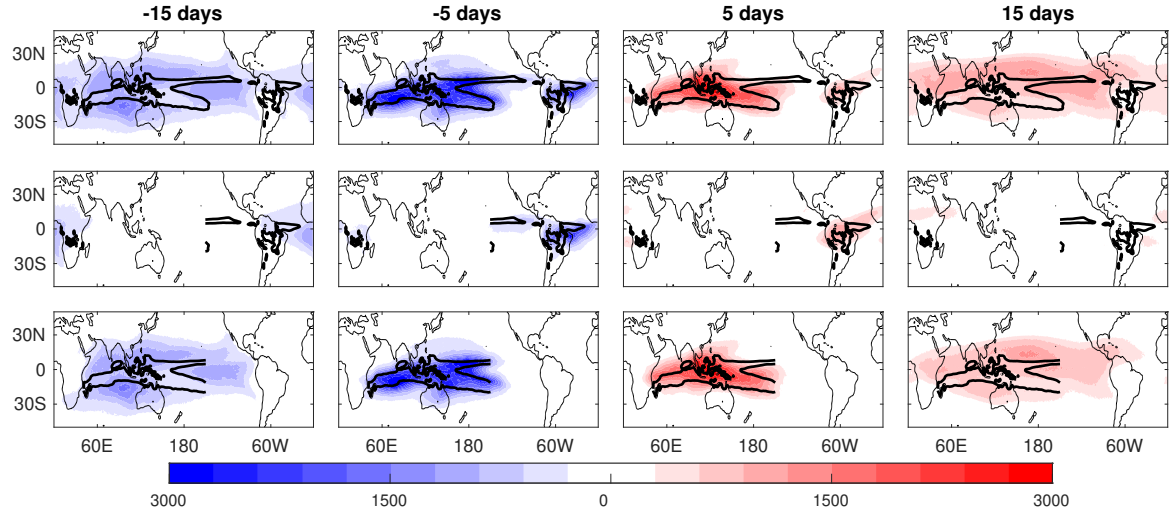

Figure 4.6: Same as Fig. 4.5, for January.

the density of trajectories in January (Fig. 4.6). Air parcels move west, then north and to the east. The East Pacific and Atlantic air parcels show limited motion corresponding to the second weaker and smaller overturning cell exhibited in the longitudinally dependent meridional circulation (Fig. 4.2). The Indo-Pacific air parcels again show that the Indo-Pacific is the driver of the circulation due to their stronger movement.

4.3 Combined Eulerian and Lagrangian analysis

The fact that the main features of the mean flow climatological trajectories (Fig. 4.3) are exhibited in the density of the forty years hourly trajectories, reassures the use of the mean flow trajectories as a representation of the main path of air parcels. To further clarify the contribution of each component of the velocity field to the actual movement of air, we plot the contribution from the different velocity components at the locations of the air parcels in the mean flow trajectories in July (Fig. 4.7). Note that the locations are a function of height

(pressure), in addition to the latitude-longitude location. The horizontal wind is decomposed using Eq. 3.1-3.3, while the decomposition of the vertical velocity is calculated following the notation of Schwendike et al. (2014).

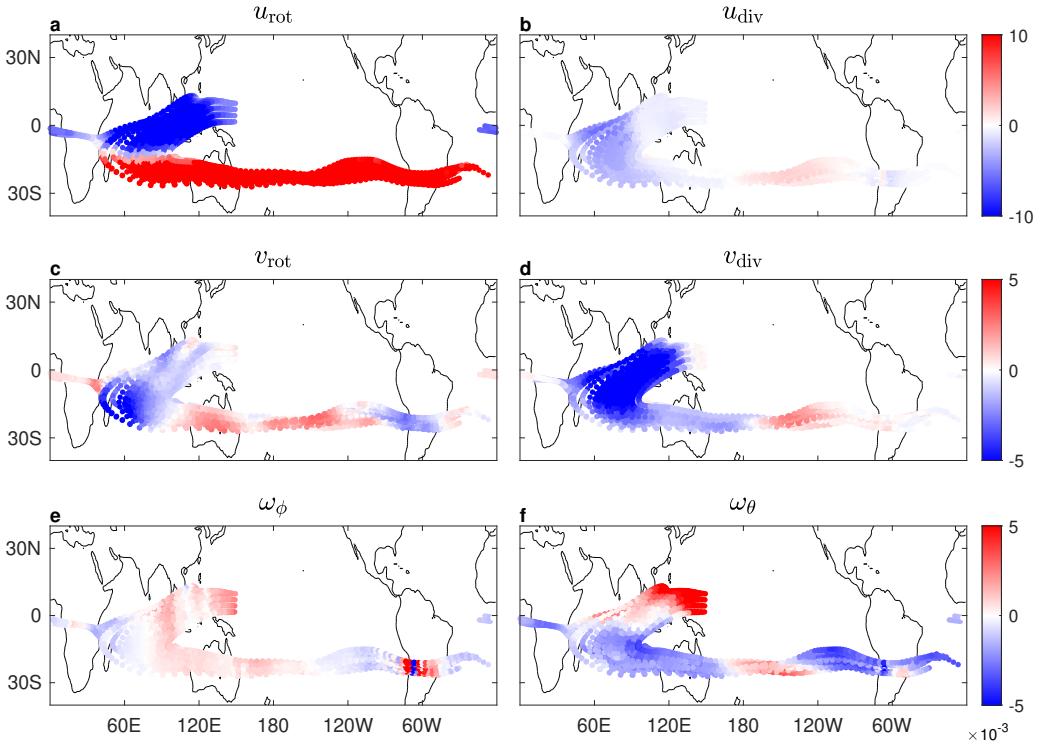

Figure 4.7: Contribution of each component of the decomposed velocity field to the mean flow movement in July, at the locations of the air parcels shown in Fig. 4.3. Color indicates the magnitude of the velocity component in $\mathrm{m\,s^{-1}}$ ($\mathrm{Pa\,s^{-1}}$) for the horizontal (vertical) wind. $(u_{\mathrm{rot}}, v_{\mathrm{rot}})$ and $(u_{\mathrm{div}}, v_{\mathrm{div}})$ are the rotational and divergent components of the horizontal wind, respectively. u_{div} participates only in the zonal circulation, and v_{div} participates only in the meridional circulation. ω_ϕ is the component of the vertical velocity that participates in the zonal circulation, and ω_θ is the component of the vertical velocity that participates in the meridional circulation.

The rotational component of the zonal flow (u_{rot}) is the strongest of all the components (Fig. 4.7a), dominating the easterlies near the equator and the jet-stream at approximately 25°S. The contribution of the divergent component of the zonal wind (u_{div}), which participates in the zonal circulation is relatively small (Fig. 4.7b), therefore, both for the initial westward motion and for the eastward motion along the jet-stream, the dominating path of air parcels is almost entirely due to the rotational zonal wind. The meridional wind, on the other hand, shows a very different behavior (Fig. 4.7c-d). The divergent component of the meridional velocity (v_{div}) dominates the movement to the south after the initial ascent near the equator. The rotational component of the meridional wind (v_{rot}), is much weaker than the divergent component in the same region, with some contribution at the most western part of the southward movement. Along the jet-stream the flow oscillates latitudinally, with similar significance to both v_{rot} and v_{div}. Note that the variations in v_{div} show the longitudinal dependence of the meridional circulation. Lastly, The component of the vertical wind (Fig. 4.7e-f) that participates in the meridional circulation (ω_θ) is much more dominant than the component that participates in the

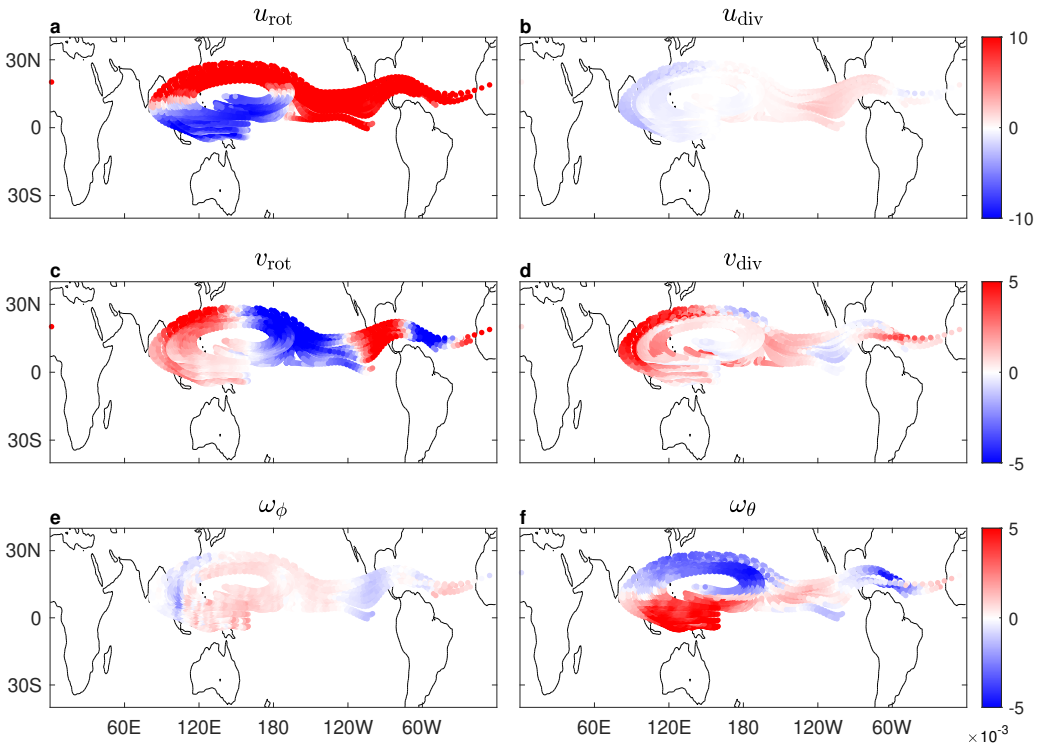

Figure 4.8: Same as Fig. 4.7, for January.

zonal circulation (ω_ϕ), in accordance with the regional Walker circulation being weaker than the regional Hadley circulation (Schwendike et al., 2014).

As expected, at the initial position of the air parcels (Fig. 4.3, black dots) there is contribution from both components to the ascending motion that generates a stronger upward motion. Interestingly, the meridional circulation, ω_θ, dominates the downward motion at 25°S, with a moderate contribution at 120°E-180°, and a stronger region at 120°W-60°W, and it also exhibits mild upward wind at 180°-120°W. Therefore, it is apparent that the decent of the air is dominated by the meridional circulation, with most of it happening close to the Americas and some in the Australian region (this is also apparent in Fig. 4.3a). Still, even in regions of weak meridional circulation, there is descent of air in the subtropics, resulting in the existence of subtropical deserts far from the regions of the strongest circulation.

In January (Fig. 4.8), the components of the velocity field feature similar relationships between each other as in July. However, one notable difference is the significance of v_{rot} with respect to v_{div}. In January, the magnitude of v_{rot} in some regions is as dominant as, or even more dominant than, v_{div}, which explains the veering of half of the trajectories southward (Fig. 4.3b).

Chapter 5

Results- CMIP5 simulations

The importance of the HC to the Earth's climate is well established, therefore, the regionality of the circulation that is found in the analysis of the present tropical large-scale circulation, can have a significant impact on the variations of the circulation under climate change. Furthermore, most of the past studies that examine the variations in the circulation under climate change used the traditional definition of the zonally averaged meridional circulation, hence there is little information about how the circulation changes in different regions. Here, we analyze these regional changes, using the coupled Eulerian-Lagrangian approach that we used for the present-day climate, but for analyzing simulations of climate change models. Combining the two approaches we are able to analyze the regional variations in different components of the circulation, as well as understand how the actual 3D movement of air parcels is expected to change in different regions, under climate change. Finally, we explain the expected changes in precipitation and their connection to the changes in the circulation.

5.1 Eulerian approach

The width of the annually averaged mean meridional circulation is similar in all 17 models we use (Fig. 5.1), and most of them agree on the poleward expansion of the HC. The multi-model mean of the mean meridional circulation (Fig. 5.2), shows an expansion of the HC, with increase of CO_2 (the RCP 8.5 scenario compared with the historical simulation). The expansion is most significant in the southern hemisphere in the annual mean and in July. In January, there is a poleward expansion of the northern HC though it is less significant. This definition of the zonally averaged HC and the zonally averaged expansion is the prediction found in previous studies for the projected changes in the circulation (e.g., Lu et al., 2007; Nguyen et al., 2015; Waugh et al., 2018; Staten et al., 2012). However, when examining the longitudinally dependent meridional circulation, the expansion occurs in specific regions only, where the circulation is less relevant (Staten et al., 2019). Therefore, the changes of the circulation as presented in the zonal mean (Fig. 5.2), where it seems that a $\sim 1^\circ - 2^\circ$ expansion occurs everywhere in the tropics in the winter hemisphere, are misleading. Taking the Eulerian approach, the longitudinally dependent meridional circulation in July is obtained as function of longitude and

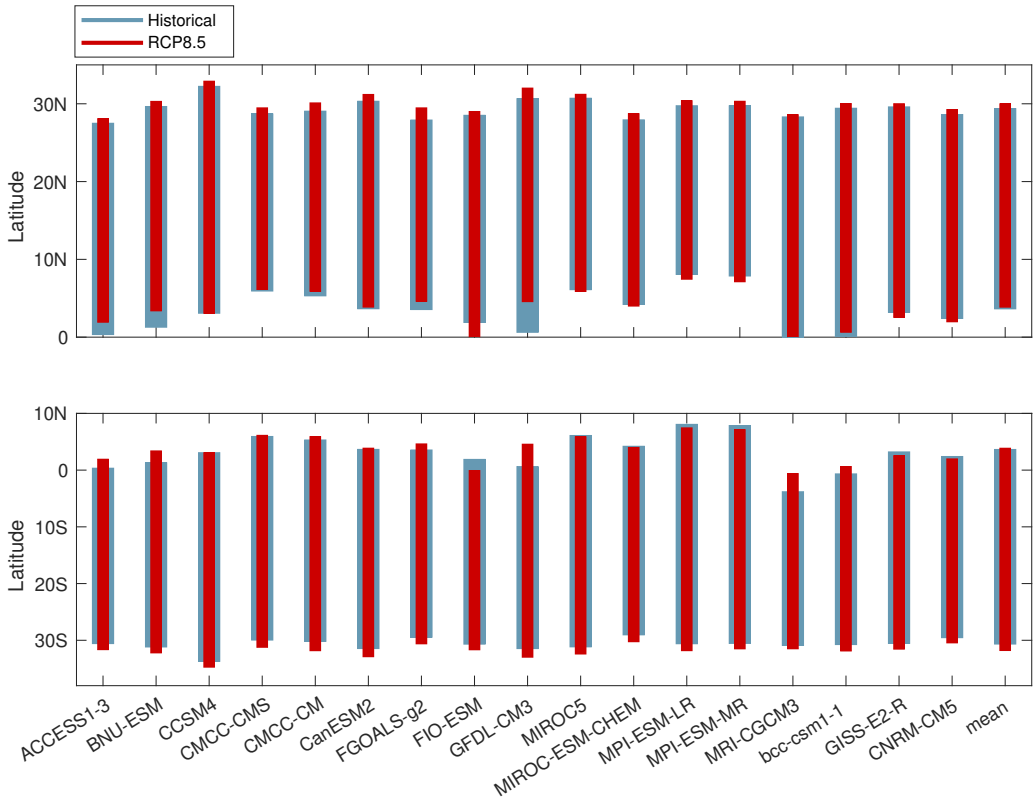

Figure 5.1: Width of the annually averaged HC for each model. The edge of the cell is defined as the latitude of the zero crossing of the mean meridional circulation at 500 hPa. Blue rectangle represents the historical (1960-1999) data and the Red rectangle represents the RCP8.5 data (2060-2099).

latitude at 500 hPa (Fig. 5.3a) for the historical data (colored contours) and the RCP 8.5 data (black contours). The air ascends and descends in the white areas and the ascending branch of the meridional circulation moves south for negative values (blue contours, and dashed black contours) and north for positive values (orange contours and solid black contours), and the opposite for the descending branch.

The variations of the circulation in longitude are very prominent, there is one very strong cell between 60°E and 180°, while in other regions the circulation is significantly weaker. Projected changes under RCP 8.5 scenario (Fig. 5.3b) are calculated as the differences between the RCP 8.5 circulation and the historical circulation and presented with the historical values for reference. In addition, the edge of the circulation is presented as the contour of the 20% of the maximum or minimum value of the historical circulation (dotted bold line) and RCP 8.5 circulation (solid bold line) at 500 hPa.

Overall, the circulation weakens under climate change, and the strongest weakening occurs in the Indo-Pacific region, where the circulation is the most prominent. Strengthening of the circulation and expanding of the cell occur between 160°W and 110°W, where the historical circulation is extremely weak, even nonexistent. While for the zonal mean meridional circulation the expansion is $\sim 1^\circ - 2^\circ$, the expansion and shrinking in the longitudinally dependent meridional circulation can reach up to $\sim 20^\circ$. Thus, the expansion of the circulation as presented in previous studies, and exhibited in the mean meridional circulation (Fig. 5.2), does not apply

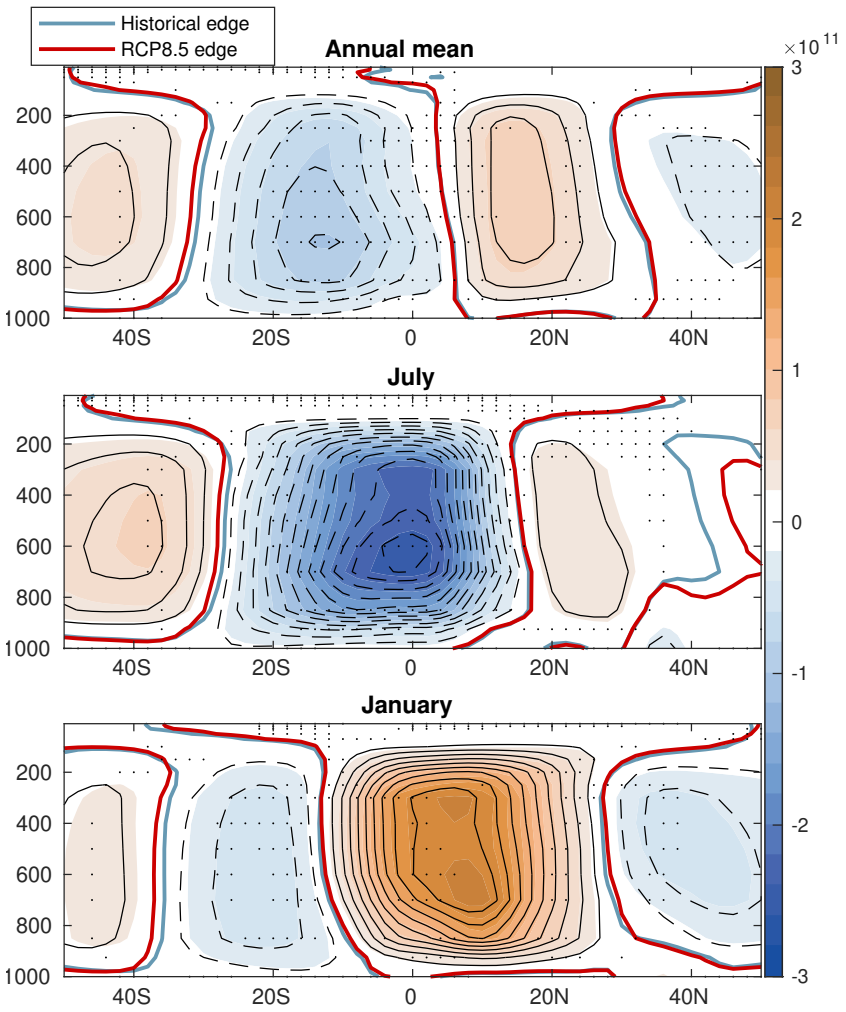

Figure 5.2: The 40-yr average of the zonally averaged meridional circulation calculated from historical (1960-1999, colored contours) and RCP8.5 (2060-2099, black contours) data from eight models. The bold solid line represent the latitude of the zero crossing of the circulation for historical and RCP8.5 (Blue and red, respectively). Colored contour interval is 0.2×10^{11} and black contour interval is 0.4×10^{11}. Dots indicate areas that are not statistically significant, at the 95% confidence level.

globally and should not be considered as prediction of the circulation under climate change. In order to obtain a more accurate picture of the changes in the large-scale circulation, the regionality must be taken into account. Moreover, since in reality the flow field is three-dimensional, the meridional circulation alone cannot account for a full, descriptive understanding of the actual changes of the entire circulation under climate change.

The actual movement of air parcels, participating in the large-scale tropical circulation, is affected by all components of the velocity field, and described as a conveyor belt, where the Indo-Pacific Warm-pool acts as the engine of the circulation (Raiter et al., 2020). Therefore, we examine other components of the circulation, which take part in the tropical conveyor belt. The latitudinally dependent zonal circulation in July is presented similarly to the meridional circulation (Fig. 5.3c), where air ascends and descends in the white areas, and the ascending branch moves west for negative values (blue contours, and dashed black contours) and east for positive values (orange contours and solid black contours). Projected changes are again

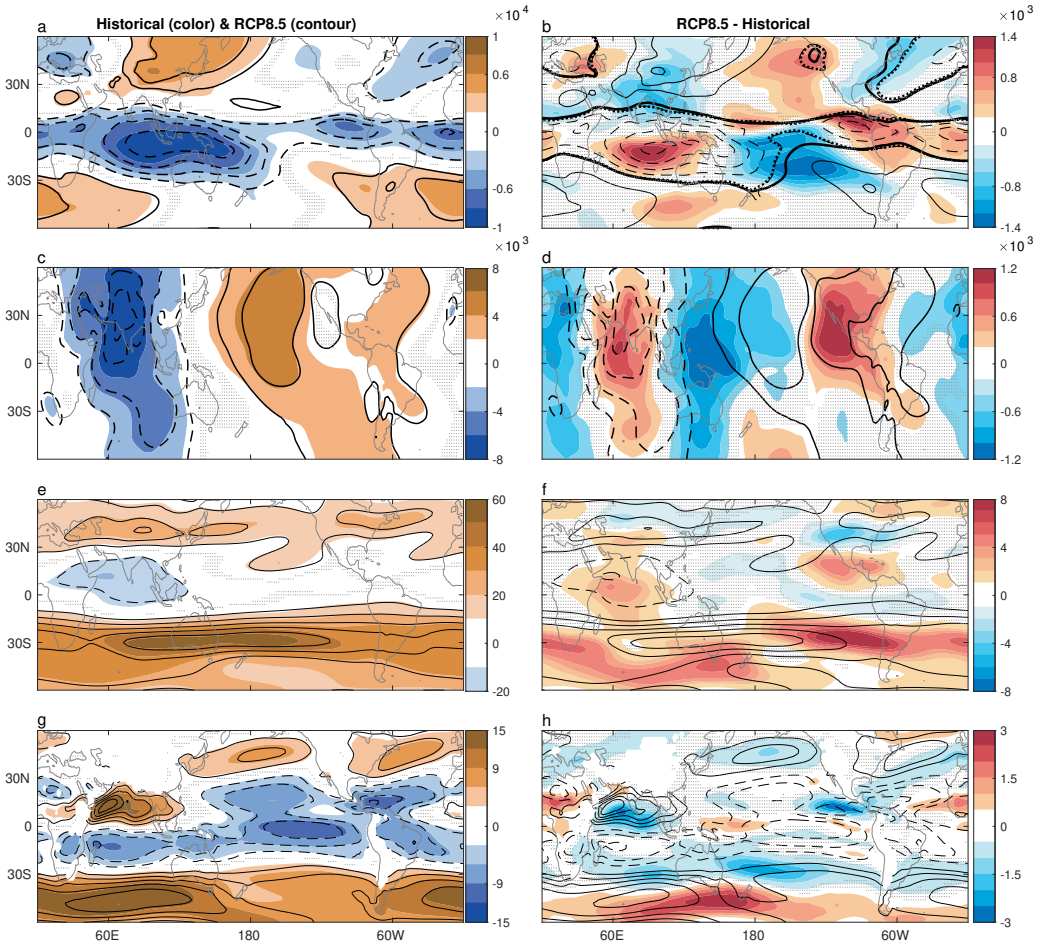

Figure 5.3: 40-yr average of components of the circulation calculated from historical (1960-1999) and RCP 8.5 (2060-2099) multi-model averaged data (left panels) and projected changes (RCP 8.5 minus historical, right panels) in July. Historical and RCP 8.5 meridional (a) and zonal (c) circulation presented in colored contours (historical) and black contours (RCP 8.5). Colored contour interval is $2 \times 10^3\,\mathrm{kg\,s^{-1}m^{-1}}$, black contour interval is $2 \times 10^3\,\mathrm{kg\,s^{-1}m^{-1}}$. Projected changes (b,d) are presented in colored contours with interval of $0.2 \times 10^3\,\mathrm{kg\,s^{-1}m^{-1}}$ with the historical values in black contours, and the 20% of the maximum value is marked with bold dashed black line for the historical and black solid line for RCP 8.5. The zonal wind at 200 hPa (e) and 850 hPa (g) for historical data (colored contours) and RCP8.5 data (black solid and dashed contours). (e): Colored contour interval is $10\,\mathrm{m\,s^{-1}}$ and black contour interval is $10\,\mathrm{m\,s^{-1}}$. (g): Colored contour and black contour interval is $3\,\mathrm{m\,s^{-1}}$. Projected changes are presented (f, h, colored contours) with the historical zonal wind (black solid and dashed contours) for reference. (f): Colored contour interval is $1\,\mathrm{m\,s^{-1}}$ and black contour interval is $10\,\mathrm{m\,s^{-1}}$. (h): colored contour interval is $0.5\,\mathrm{m\,s^{-1}}$ and black contour interval is $3\,\mathrm{m\,s^{-1}}$. Dots indicate areas that are not statistically significant, at the 95% confidence level.

presented with the historical values (Fig. 5.3d). Changes in the zonal circulation are more significant than in the meridional circulation, and the most noticeable feature is shifting of the circulation to the east, detected in the location of the ascending branch for the historical and RCP 8.5.

Next, we examine the zonal wind due to the strong contribution of the jet-stream and the easterlies to the air parcels' movement. The zonal wind is presented at 200 hPa (Fig. 5.3e) and at 850 hPa (Fig. 5.3g) for the historical data (colored contours) and the RCP 8.5 data

(black contours). Projected changes are presented with the historical zonal wind for reference (Fig. 5.3f,h, colored contours and black contours, respectively). The jet-stream strengthens significantly with the increase of CO_2, while the easterlies are weakening.

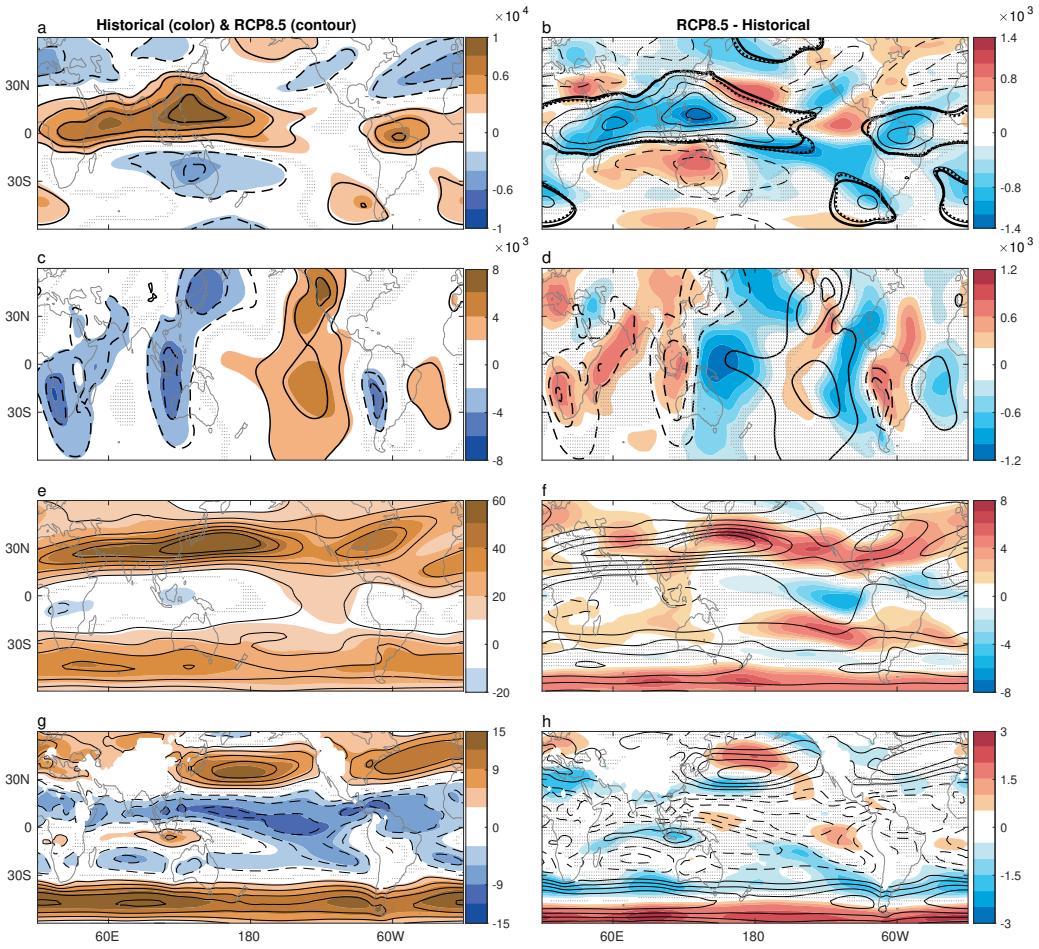

Figure 5.4: Same as in Fig. 5.3, for January.

In January the weakening of the circulation is even more prominent than in July, and the Indo-Pacific region is again the region where the most significant weakening occurs. Strengthening of the circulation occurs in the descending branch at $\sim 180°$, where the edge of the circulation expands northward. In the zonal circulation, there is again, shift eastward of the ascending regions (Fig. 5.3c,d), and the zonal wind shows strengthening of the jet-stream and weakening of the easterlies (Fig. 5.3e-h).

Analyzing each component separately is useful for understanding the different contributions of the components to the actual changes in the circulation under climate change. However, this Eulerian analysis is lacking in visualizing how all components together affect the actual movement of the air parcels. Hence, we use a Lagrangian method, following the path of the air parcels.

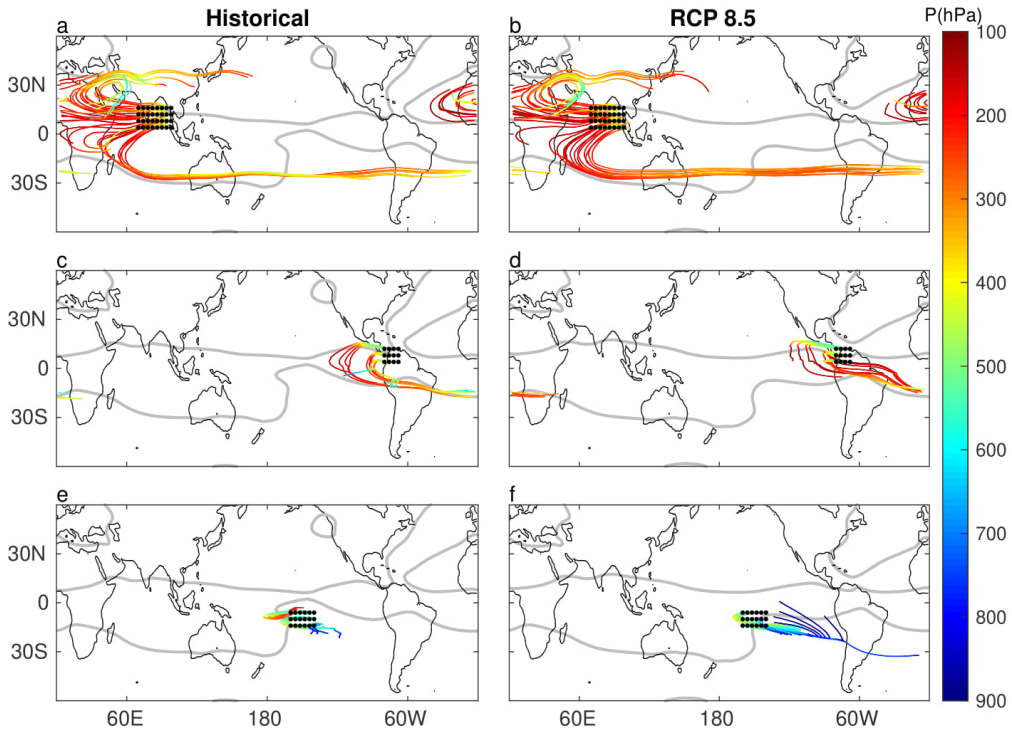

Figure 5.5: Mean flow trajectories for July calculated from eight models using historical (left panel) and RCP 8.5 (right panels) data. The lines show the air parcels trajectories going 20 days forward in time. The initial locations are marked with black dots. The color of the lines indicates the pressure level in hPa. Gray solid line is the 20% from the maximum contour of the meridional circulation for the historical and RCP 8.5 data accordingly.

5.2 Lagrangian approach

We use the climatological flow to calculate the trajectories of air parcels initially positioned in three example regions, both for the historical data and RCP 8.5 data (Fig. 5.5), allowing a comparison of the three-dimensional motion of air between the two data sets. The initial positions of the air parcels are marked with black dots and we track each air parcel for 20 days, color indicates height.

First, we position air parcels where the air moves in the tropical conveyor belt (Fig. 5.5a,b). In both data sets, the air ascends, moves to the west and poleward, before merging into the jet-stream and moving east. The air parcels are initially located where there is strengthening of the meridional circulation and northward expansion of the cell (Fig. 5.3 b). Dissimilarities are found in the beginning of the trajectories, the historical air parcels move stronger to the west and northward, while RCP 8.5 trajectories move to the south, coinciding with strengthening of the meridional circulation, as well as weakening of the easterly wind at 200 hPa and of the zonal circulation (Fig. 5.3d,f). Another dissimilarity arises due to the strengthening of the jet stream, the historical air parcels in the jet stream descend earlier than the RCP 8.5 air parcels.

The second region is in Central America and the northern part of South America (Fig. 5.5c,d). In this region, the meridional circulation is weak and the movement of the air parcels is very localized. The motion is confined to the edge of the meridional circulation (gray contour), and therefore the historical air parcels move more to the south. In this region the circulation is

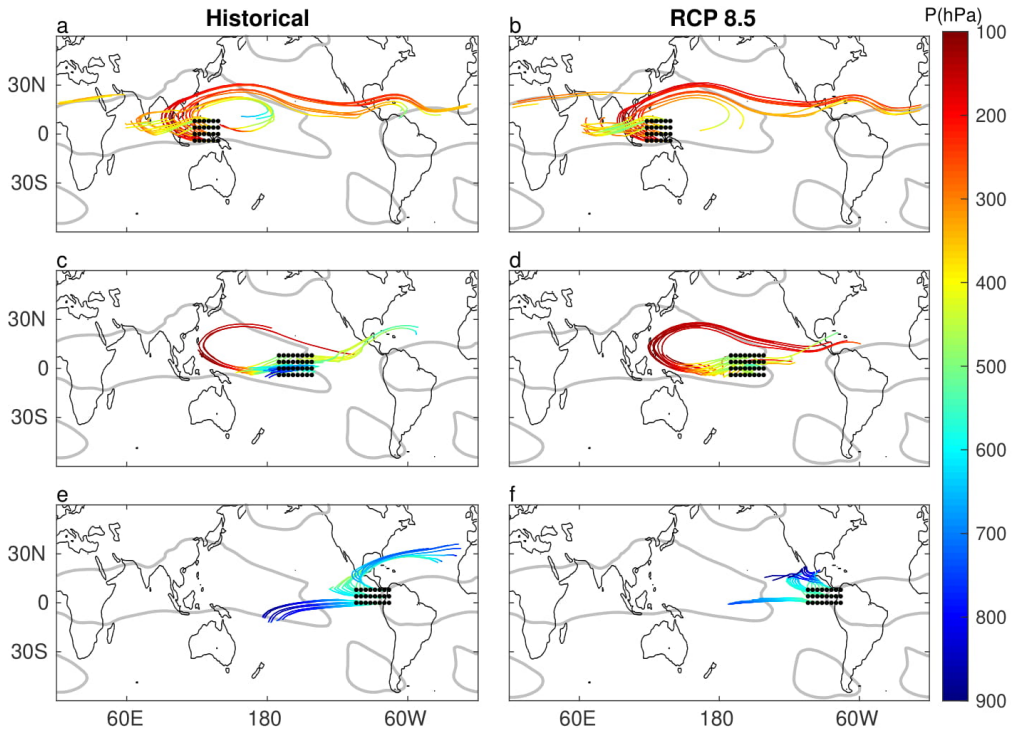

Figure 5.6: Same as Fig. 5.5, for January.

shrinking rather than expanding.

Lastly, we examine the region where the expansion of the cell is most significant, in the center of the Pacific Ocean (Fig. 5.5e,f). For the historical data, the circulation does not exist in this region and indeed the trajectories show a very limited motion, where some air parcels even ascend. However, due to the expanding of the circulation under RCP 8.5 scenario, now this region is inside the edge of the cell and the air parcels move with the descending branch, meaning to the north.

We present three additional examples for January (Fig. 5.6). The First (a,b), shows the change in the air movement in the tropical conveyor belt, where the strengthening of the jet-stream is apparent (Fig. 5.4). The second example (Fig. 5.6c,d) is at the center of the Pacific, where there is strengthening of the circulation where it was weak in the past. All air parcels in this region appear to be participating in the circulation in the RCP 8.5 scenario, while most of the historical air parcels move very locally and descend. The third example (Fig. 5.6e,f), where the weakening of the circulation and the zonal velocity in the RCP 8.5 scenario is visible.

5.3 Changes in precipitation flux

The large scale circulation and precipitation are physically connected due to the ascent of air in the large-scale tropical circulation which creates a zone of high rainfall, while the location of the descent of air in the circulation usually coincides with arid regions (Fig. 5.7c). The mechanisms controlling the changes of the precipitation under climate change are strongly dependent on the region of interest. Some regions experience the classic “wet gets wetter” outcome (Held and Soden, 2006; Chou et al., 2009), while other regions respond differently, partially due to

changes in the circulation (Vecchi and Soden, 2007; Seager et al., 2010).

We use the Helmholtz decomposition to decompose the vertical velocity into ω_θ, associated with the meridional circulation, and ω_ϕ, associated with the zonal circulation (Keyser et al., 1989; Schwendike et al., 2014). The changes in the decomposed vertical velocity, presented at 500 hPa (Fig. 5.7a,b), represent the contribution of each component of the circulation to the local ascent and descent of air.

Changes in precipitation flux between the historical and RCP 8.5 data (Fig. 5.7d) show regions that coincide with the "wet gets wetter" theory, for example, the monsoon region in South-East Asia. However, some regions show a very different response, where wet gets drier and dry gets wetter. For example, in the Indo-Pacific region, there is a drying response in the RCP 8.5 scenario, even-though this region was considered a wet region in the historical data. This drying coincides with weakening of the ascent of air in the same region both in ω_θ and ω_ϕ. Another region of interest is in the center of the Pacific, which was discussed earlier in this study (Fig. 5.5, bottom panels). Where the circulation did not exist in the past, we see a significant strengthening of the precipitation flux, although, in the historical simulation the precipitation flux was weak, hence, dry gets wetter. This response again coincides with the changes in the vertical velocity.

Precipitation changes in other regions agree as well with the changes in the vertical velocity, more with ω_θ, associated with the meridional circulation, than with ω_ϕ, associated with the zonal circulation. For example, drying in Central America corresponding with weakening of the ascent in the same area (Fig. 5.7a), and drying in South Australia, corresponding with strengthening of the descent at the edge of the meridional circulation (marked with gray contours).

The response of the precipitation in January is very similar to the response in July. There is strengthening of the precipitation flux at the ascending branch of the meridional circulation (Fig. 5.8,d). Similarly to July, the ascent at the center of the Pacific strengthens, where no circulation existed in the historical data, resulting in an intensification of the precipitation. Weakening at the Indo-pacific region is apparent in January as well.

Previous studies used the traditional definition of the zonal mean meridional circulation, and referred to any zonal asymmetry as part of the Walker circulation (Seager et al., 2010; Vecchi and Soden, 2007). Therefore, when discussing the contribution of the dynamical component to the changes in precipitation, zonally asymmetric dynamical changes were attributed to the weakening of the Walker circulation alone. However, when inspecting the decomposed vertical components (Fig. 5.7,5.8 a,b), it is very clear that the meridional component has a strong contribution to the precipitation change, even stronger than the contribution of the zonal component. This highlights a difficulty with the traditional definition of the large-scale circulation. The understanding of the complicated mechanism of precipitation change in the tropics was limited due to disregarding the regionality of the meridional circulation, and the fact that it is connected to the zonal and horizontal components as well. Moreover, when combining the different components of the circulation, to a conveyor belt definition, we can see a

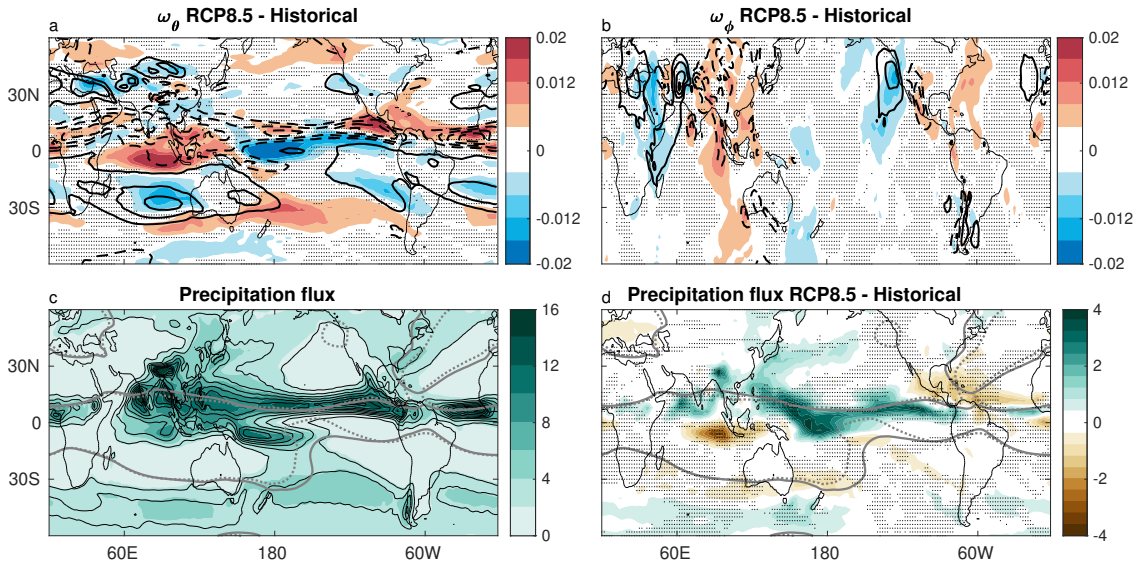

Figure 5.7: Changes in the decomposed vertical velocity (a,b, colored contours) in July. Black contours represent the historical values for reference. Colored contour interval is $4\times10^{-3}\,\mathrm{Pa\,s^{-1}}$, and black contour interval is $2\times10^{-2}\,\mathrm{Pa\,s^{-1}}$. ω_ϕ is the component of the vertical velocity that participates in the zonal circulation, and ω_θ is the component of the vertical velocity that participates in the meridional circulation. Precipitation flux (c) of the historical (colored contours) and RCP 8.5 (black contours) data for July is presented with contour interval of 2 mm/day. Changes in precipitation flux (RCP 8.5 - Historical, d) in July are presented with contour interval of 0.4 mm/day. Positive (negative) values indicate stronger (weaker) flux in the RCP 8.5 scenario. Dots indicate areas that are not statistically significant, at the 95% confidence level.

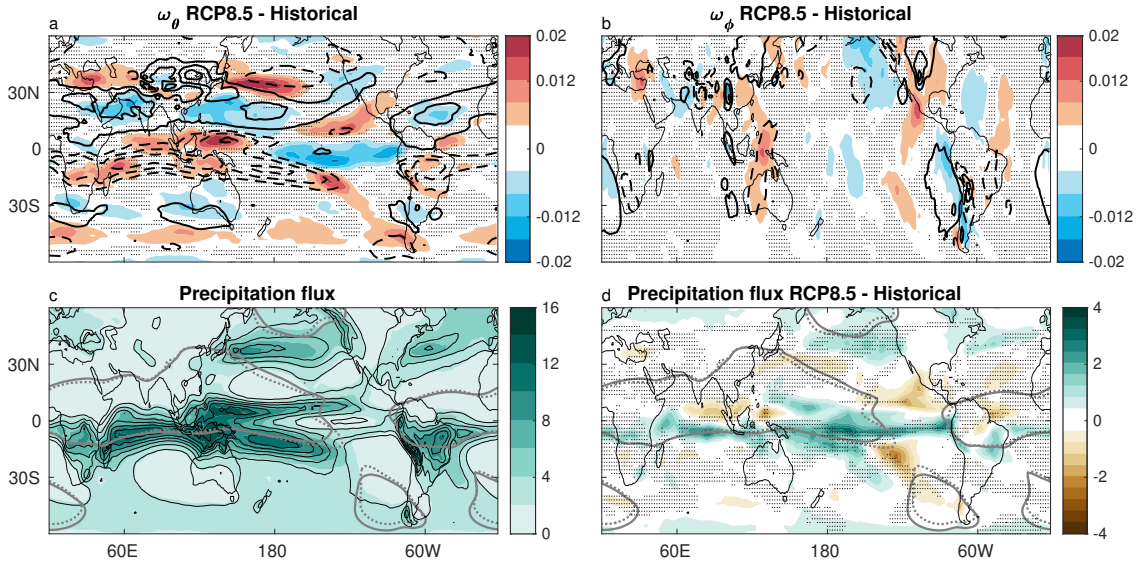

Figure 5.8: Same as Fig. 5.7, for January.

shift in the ascending region of this conveyor belt. Both in January and July, there is weakening of the ascent at the Indo-Pacific region (Fig. 5.7,5.8 a,b), in both components of the vertical velocity. On the other hand, there is strengthening of the ascent east to the Indo-Pacific region at the center of the Pacific, creating a shift in the vertical motion that translates to changes in precipitation. Both in July and in January, there is weakening of the precipitation in the Indo-pacific region and intensification at the center of the Pacific.

Chapter 6

Discussion

The large scale circulation in the tropics is traditionally described in terms of the Hadley circulation, a definition that does not take into account variability with longitude. In the past decade, studies have shown that the circulation strongly depends on the longitudinal position (e.g., Schwendike et al., 2014; Nguyen et al., 2018; Karnauskas and Ummenhofer, 2014), raising the question of how does the air actually circulate in the tropics. In this study, we revisit this question by using a combination of Eulerian and Lagrangian analyses.

Decomposing the velocity field into rotational and divergent components, we analyze the longitudinal dependence of the tropical circulation. The strong variations in longitude (Fig. 4.1) motivate inspection of the actual movement of air in the tropical atmosphere, i.e., to analyze the velocity field with a Lagrangian approach. Calculating trajectories of the mean flow reveals

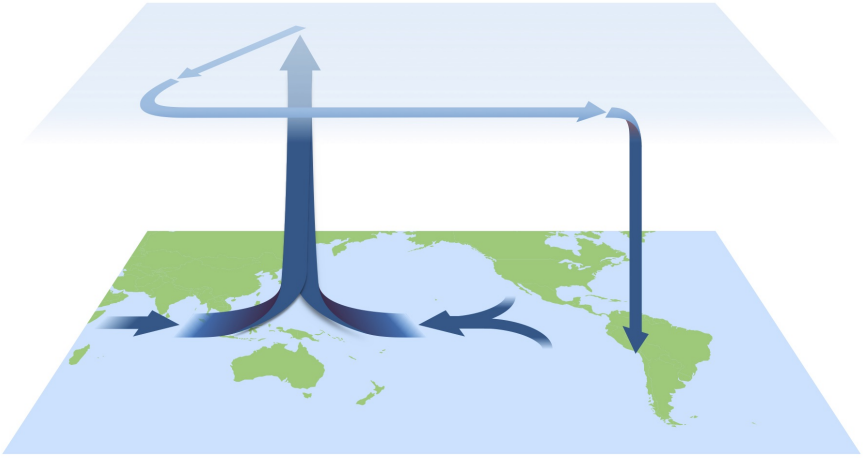

Figure 6.1: A schematic of the dominant path of air parcels participating in the large scale tropical conveyor for July. The air parcels converge into the Indo-Pacific, ascend, move to the west and to the south, merge into the jet stream and move east, eventually descending near the Americas.

a complex pattern, involving all components of the velocity field (Fig. 4.3). This pattern is also exhibited in the density of trajectories (Fig. 4.5). Looking at the distribution of the air parcels, it is noticeable that the circulation is indeed regional, where the Indo-Pacific region is the driver of the circulation. Furthermore, we find that all components of the decomposed velocity field contribute significantly to the circulation.

Combining the Eulerian and Lagrangian approaches, we are able to analyze the circulation in the tropics considering all aspects of the circulation, without any presumptions. The Eulerian analysis gives information about the different types of circulations (rotational, meridional and zonal) isolated from one another, making it easy to understand the contribution of each component to the entire circulation. The Lagrangian analysis, on the other hand, compiles all components to a 3D pattern of the circulation, where the effect of each component is visible in the air parcels' paths. Hence, although it is useful to decompose the circulation into different components, in reality, all components are required to explain the motion of air. This is further established when exploring the contribution of the different components of the velocity field at the locations of air parcels in the mean flow trajectories (Fig. 4.7).

The combined Eulerian-Largangian analysis, that takes into account all the components of the velocity field, reveals a circulation pattern in the tropics that can be described as a conveyor belt (Fig. 6.1). Air converges into the Indo-Pacific Warm Pool which acts as the engine of the circulation. This air ascends, moves westward in the upper layers with the rotational winds, and then poleward with the meridional circulation. It reaches approximately 25°S (or 25°N in the opposite season), merges into the jet-stream and moves rapidly to the east. Finally, it descends near the Americas. This new definition more accurately represents the circulation in the tropics, and shows the regionality and three-dimensionality of the circulation as manifested in the Eulerian and Lagrangian analyses.

In the second part of this study, we investigate the response of the tropical circulation to climate change and its impact on the precipitation changes. While the HC was found to be expanding under climate change scenarios, recent studies found that this expansion is rather regional, and occurs mostly where the circulation is insignificant. Here, we look into the decomposed circulation and show that indeed, the expansion is regional, and in some regions the circulation shrinks or does not experience change in its width. These results, accompanied by the three-dimensionality of the actual flow, motivate us to investigate other components of the circulation apart from the meridional circulation. The Helmholtz decomposition allows us to do so - analyze the different components separated from one another. We found that both the zonal and the meridional decomposed circulations exhibit regional dissimilarities. The zonal wind, on the other hand, exhibits a cohesive trend.

The Eulerian analysis establishes the regional changes in each component of the circulation. The meridional circulation is weakening and the expansion occurs where the historical circulation did not exist, i.e., a region that was in the past outside of the HC and, in the future, will be a part of it. The zonal circulation is found to move to the east, changing the regions of ascent and descent of air. The zonal wind shows strengthening of the jet-stream and weakening

of the easterlies. However, it is unclear, from this analysis alone, how the actual movement of air in the atmosphere will change.

The Lagrangian analysis is then used, to visualize the changes in the actual three-dimensional movement of air by calculating trajectories of air parcels. Choosing three examples for initial positions, the contribution of each component of the circulation to the actual flow is apparent and the response of the flow to climate change can be examined. We found that all components contribute to the three-dimensional flow, and indeed, different regions respond differently.

The trajectories initially located in the center of the Pacific Ocean agree with the decomposed meridional circulation. This region, where the circulation did not exist in the past, will be inside the descending branch of the HC. This leads to significant changes in precipitation since the descending branch of the HC coincides with arid regions. This example, and the two others presented here, emphasize the importance of regional analysis of the response of the flow to climate change.

When addressing the changes in the circulation in terms of the tropical conveyor belt, we identify a shift to the east of the ascending region of the conveyor belt. The ascent located at the Indo-Pacific region weakens under climate change and the ascent of air at the center of the Pacific strengthens. This shift enhances ascent of air where the historical circulation did not exist, causing intensification of the precipitation.

Bibliography

Back, L. E. and Bretherton, C. S. (2006). Geographic variability in the export of moist static energy and vertical motion profiles in the tropical pacific. *Geophys. Res. Lett.*, 33(17).

Chadwick, R., Boutle, I., and Martin, G. (2013). Spatial patterns of precipitation change in cmip5: Why the rich do not get richer in the tropics. *J. Climate*, 26(11):3803–3822.

Chemke, R. and Polvani, L. M. (2019a). Exploiting the abrupt 4×CO2 scenario to elucidate tropical expansion mechanisms. *J. Climate*, 32(3):859–875.

Chemke, R. and Polvani, L. M. (2019b). Opposite tropical circulation trends in climate models and in reanalyses. *Nature Geoscience*, 12(7):528–532.

Chou, C., Neelin, J. D., Chen, C.-A., and Tu, J.-Y. (2009). Evaluating the "rich-get-richer" mechanism in tropical precipitation change under global warming. *J. Climate*, 22(8):1982–2005.

Chou, C., Wu, T.-C., and Tan, P.-H. (2013). Changes in gross moist stability in the tropics under global warming. *Clim. Dyn.*, 41(9):2481–2496.

D'Agostino, R., Scambiati, A. L., Jungclaus, J., and Lionello, P. (2020). Poleward shift of northern subtropics in winter: Time of emergence of zonal versus regional signals. *Geophys. Res. Lett.*, 47(19):e2020GL089325.

Davis, N. and Birner, T. (2017). On the discrepancies in tropical belt expansion between reanalyses and climate models and among tropical belt width metrics. *J. Climate*, 30(4):1211–1231.

Davis, S. M. and Rosenlof, K. H. (2012). A multidiagnostic intercomparison of tropical-width time series using reanalyses and satellite observations. *J. Climate*, 25(4):1061–1078.

Dee, D. et al. (2013). The ERA-Interim reanalysis: configuration and performance of the data assimilation system. *Q. J. R. Meteorol. Soc.*, 137(656):553–597.

Diaz, H. F. and Bradley, R. S. (2004). *The Hadley Circulation: Present, Past, and Future*, pages 1–5. Springer Netherlands, Dordrecht.

Dima, I. M. and Wallace, J. M. (2002). Notes and correspondence on the seasonality of the Hadley cell. *J. Atmos. Sci.*, 60:1522–1527.

Grise, K. M., Davis, S. M., Simpson, I. R., Waugh, D. W., Fu, Q., Allen, R. J., Rosenlof, K. H., Ummenhofer, C. C., Karnauskas, K. B., Maycock, A. C., Quan, X., Birner, T., and Staten, P. W. (2019). Recent tropical expansion: Natural variability or forced response? *J. Climate*, 32(5):1551–1571.

Hartmann, D. L. (2016). Chapter 6 - Atmospheric general circulation and climate. In *Global Physical Climatology (Second Edition)*, pages 159 – 193. Elsevier, Boston, second edition edition.

Held, I. M. and Hou, A. Y. (1980). Nonlinear axially symmetric circulations in a nearly inviscid atmosphere. *J. Atmos. Sci.*, 37:515–533.

Held, I. M. and Soden, B. J. (2006). Robust responses of the hydrological cycle to global warming. *J. Climate*, 19(21):5686–5699.

Hu, S., Cheng, J., and Chou, J. (2017). Novel three-pattern decomposition of global atmospheric circulation: generalization of traditional two-dimensional decomposition. *Clim. Dyn.*, 49(9-10):3573–3586.

Hu, Y. and Fu, Q. (2007). Observed poleward expansion of the Hadley circulation since 1979. *Atmos. Chem. Phys.*, 7(19):5229–5236.

Kang, S. M., Deser, C., and Polvani, L. M. (2013). Uncertainty in climate change projections of the Hadley circulation: The role of internal variability. *J. Climate*, 26(19):7541–7554.

Karnauskas, K. B. and Ummenhofer, C. C. (2014). On the dynamics of the Hadley circulation and subtropical drying. *Clim. Dyn.*, 42(9):2259–2269.

Keyser, D., Schmidt, B. D., and Duffy, D. G. (1989). A technique for representing three-dimensional vertical circulations in baroclinic disturbances. *Mon. Weath. Rev.*, 117(11):2463–2494.

Lindzen, R. S. and Hou, A. V. (1988). Hadley circulations for zonally averaged heating centered off the equator. *J. Atmos. Sci.*, 45(17):2416–2427.

Lu, J., Vecchi, G. A., and Reichler, T. (2007). Expansion of the Hadley cell under global warming. *Geophys. Res. Lett.*, 34(6).

Lucas, C.and Nguyen, H. (2015). Regional characteristics of tropical expansion and the role of climate variability. *J. Geophys. Res. (Atmos.)*, 120(14):6809–6824.

Ma, J., Chadwick, R., Seo, K.-H., Dong, C., Huang, G., Foltz, G. R., and Jiang, J. H. (2018). Responses of the tropical atmospheric circulation to climate change and connection to the hydrological cycle. *Ann. Rev. Earth Plan. Sci.*, 46(1):549–580.

Ma, J. and Xie, S.-P. (2013). Regional patterns of sea surface temperature change: A source of uncertainty in future projections of precipitation and atmospheric circulation*. *J. Climate*, 26(8):2482–2501.

Menzel, M. E., Waugh, D., and Grise, K. (2019). Disconnect between Hadley cell and subtropical jet variability and response to increased CO2. *Geophys. Res. Lett.*, 46(12):7045–7053.

Neelin, J. D. and Held, I. M. (1987). Modeling tropical convergence based on the moist static energy budget. *Mon. Weath. Rev.*, 115(1):3–12.

Nguyen, H., Hendon, H. H., Lim, E. P., Boschat, G., Maloney, E., and Timbal, B. (2018). Variability of the extent of the Hadley circulation in the southern hemisphere: a regional perspective. *Clim. Dyn.*, 50(1):129–142.

Nguyen, H., Lucas, C., Evans, A., Timbal, B., and Hanson, L. (2015). Expansion of the southern hemisphere Hadley cell in response to greenhouse gas forcing. *J. Climate*, 28(20):8067–8077.

Raiter, D., Galanti, E., and Kaspi, Y. (2020). The tropical atmospheric conveyor belt: A coupled Eulerian-Lagrangian analysis of the large-scale tropical circulation. *Geophys. Res. Lett.*, 47(10):e2019GL086437.

Schwendike, J., Berry, G., Reeder, M., Jakob, C., Govekar, P., and Wardle, R. (2015). Trends in the local Hadley and local Walker circulations. *J. Geophys. Res. (Atmos.)*, 120(15):7599–7618.

Schwendike, J., Govekar, P., Reeder, M. J., Wardle, R., Berry, G. J., and Jakob, C. (2014). Local partitioning of the overturning circulation in the tropics and the connection to the Hadley and Walker circulations. *J. Geophys. Res. (Atmos.)*, 119(3):1322–1339.

Seager, R., Naik, N., and Vecchi, G. A. (2010). Thermodynamic and dynamic mechanisms for large-scale changes in the hydrological cycle in response to global warming*. *J. Climate*, 23(17):4651–4668.

Seidel, D. J. and Randel, W. J. (2007). Recent widening of the tropical belt: Evidence from tropopause observations. *J. Geophys. Res. (Atmos.)*, 112(D20).

Sprenger, M. and Wernli, H. (2015). The LAGRANTO lagrangian analysis tool version 2.0. *Geosci. Model Development*, 8(8):2569–2586.

Staten, P. W., Grise, K. M., Davis, S. M., Karnauskas, K., and Davis, N. (2019). Regional widening of tropical overturning: Forced change, natural variability, and recent trends. *J. Geophys. Res. (Atmos.)*, 124(12):6104–6119.

Staten, P. W., Lu, J., Grise, K. M., Davis, S. M., and Birner, T. (2018). Re-examining tropical expansion. *Nature Cliamte Change*, 8(9):768–775.

Staten, P. W., Rutz, J. J., Reichler, T., and Lu, J. (2012). Breaking down the tropospheric circulation response by forcing. *Clim. Dyn.*, 39(9):2361–2375.

Taylor, K. E., Stouffer, R. J., and Meehl, G. A. (2012). An overview of cmip5 and the experiment design. *Bull. Am. Meteor. Soc.*, 93(4):485–498.

Vallis, G. K. (2006). *Atmospheric and Oceanic Fluid Dynamics*. pp. 770. Cambridge University Press.

Vecchi, G. A. and Soden, B. J. (2007). Global warming and the weakening of the tropical circulation. *J. Climate*, 20(17):4316–4340.

Waugh, D. W., Grise, K. M., Seviour, W. J. M., Davis, S. M., Davis, N., Adam, O., Son, S.-W., Simpson, I. R., Staten, P. W., Maycock, A. C., Ummenhofer, C. C., Birner, T., and Ming, A. (2018). Revisiting the relationship among metrics of tropical expansion. *J. Climate*, 31(18):7565–7581.

Xie, S.-P., Deser, C.and Vecchi, G. A., Ma, J., Teng, H., and Wittenberg, A. T. (2010). Global warming pattern formation: Sea surface temperature and rainfall*. *J. Climate*, 23(4):966–986.

Zhang, G. and Wang, Z. (2013). Interannual variability of the Atlantic Hadley circulation in boreal summer and its impacts on tropical cyclone activity. *J. Climate*, 26(21):8529–8544.